Antireflection-assisted all-dielectric terahertz metamaterial polarization converter

Antireflection-assisted all-dielectric terahertz metamaterial polarization converter

Jianchen Zi, Quan Xu, Qiu Wang, Chunxiu Tian, Yanfeng Li, Xixiang Zhang, Jiaguang Han, and Weili Zhang

Citation: Appl. Phys. Lett. **113**, 101104 (2018); doi: 10.1063/1.5042784
View online: https://doi.org/10.1063/1.5042784
View Table of Contents: http://aip.scitation.org/toc/apl/113/10
Published by the American Institute of Physics

Antireflection-assisted all-dielectric terahertz metamaterial polarization converter

Jianchen Zi,[1] Quan Xu,[1] Qiu Wang,[1] Chunxiu Tian,[2] Yanfeng Li,[1,a)] Xixiang Zhang,[2] Jiaguang Han,[1,a)] and Weili Zhang[1,3,a)]
[1]*Center for Terahertz Waves, College of Precision Instrument and Optoelectronics Engineering, Tianjin University, Key Laboratory of Optoelectronic Information Technology (Ministry of Education of China), Tianjin 300072, People's Republic of China*
[2]*Division of Physical Science and Engineering, King Abdullah University of Science and Technology, Thuwal 23955-6900, Saudi Arabia*
[3]*School of Electrical and Computer Engineering, Oklahoma State University, Stillwater, Oklahoma 74078, USA*

(Received 4 June 2018; accepted 22 August 2018; published online 6 September 2018)

We present a transmissive all-dielectric terahertz (THz) metamaterial half-wave plate with a double-working-layer structure. One layer works as a half-wave plate to enable polarization conversion of the incident THz wave, and the other layer functions as an antireflection layer to improve the transmission. The device is made of pure silicon only and can realize a high-performance polarization conversion at the designed THz frequency. Numerical simulations have been performed to show how the polarization properties of the THz wave can be adjusted by the structural parameters of the metamaterial. With appropriate structural parameters, the transmission for cross-polarization can reach 90%, and the polarization conversion rate can reach almost 100% at the designed operation frequency of 1 THz in simulation. Several samples have been fabricated and characterized, and the experimental results show a cross-polarized transmission of about 80% and a polarization conversion rate of almost 100% and agree well with the simulations. *Published by AIP Publishing.*
https://doi.org/10.1063/1.5042784

Terahertz (THz) waves usually refer to the electromagnetic (EM) waves within the frequency band of 0.1–10 THz. Thanks to their unique physical properties, THz waves have been widely applied in various fields such as imaging,[1] spectroscopy,[2] and communications.[3] However, the lack of efficient THz functional devices such as modulators,[4–6] sensors,[7,8] multipole oscillators/microcavities,[9,10] filters,[11,12] absorbers,[13–15] and splitters[16] still hinders the rapid development of the THz technology.

Wave plates, as a basic device to modulate the polarization of EM waves, are also very important for the THz technology. Traditional wave plates use material birefringence to realize polarization conversion. However, they can hardly avoid the disadvantages of low birefringence, huge loss, and high cost.[17–19] For example, a quarter-wave plate (QWP) of crystalline quartz has a thickness over 1 mm at an operation frequency of 1 THz due to its low birefringence.[20] Obviously, bulky devices cannot satisfy the future trends of development towards miniaturization and integration.

Metamaterials are artificial materials composed of subwavelength elements.[21–25] With the help of flexible structural design, metamaterials can realize a variety of unusual properties and provide alternative solutions to solve the problems in high-performance device design in the THz band. Many THz polarization converters based on metamaterials have been reported. Reference 26 proposed an anisotropic metamaterial to work as a reflective half-wave plate (HWP) with a polarization conversion rate (PCR) over 85% in the frequency band of 0.67–1.66 THz. An HWP with a cut-wire-pair structure was designed to realize a high-amplitude helicity conversion rate over 80% at 0.5 THz.[27] Reference 28 reported a polarization converter with a transmission of 49% and a PCR of 51% at 0.66 THz based on a double-chain-ring structure metamaterial. Reference 29 achieved a cross-polarization converter based on a through-via connected double-layer slot structure with a PCR of 99.9% and a transmission over 80% in the frequency band of 0.3–1.4 THz. A reflective metamaterial was used to realize controllable polarization conversion for all polarization states at 2.32 THz.[30] The phase-change property of VO_2 was utilized to achieve a switchable THz QWP with a transmission of 59% at 0.468 THz.[31] Reference 32 described a single-layer metasurface working as an HWP with a PCR over 90% and a transmission under 30% at 0.91–1.45 THz. An all-dielectric gradient grating was proposed to realize cross-polarization conversion at 1.06 THz,[33] and its transmission and PCR can reach 69% and 99.3%, respectively. However, these metamaterial devices usually have a low transmission and PCR or work in the reflective mode, and therefore, higher performance devices are still desirable.

In this paper, we report a transmissive THz HWP based on an all-dielectric metamaterial consisting of two working layers. The working layers are fabricated on the two surfaces of a silicon wafer separately. One layer works as an HWP to convert the polarization state of the incident THz wave, and the other layer is an antireflection layer (ARL) to improve the transmission. Different from our previous work where elliptical air holes in silicon are used to achieve the birefringence,[34] the current design employs silicon pillars for

a)Authors to whom correspondence should be addressed: yanfengli@tju.edu.cn; jiaghan@tju.edu.cn; and weili.zhang@okstate.edu

birefringence, but most importantly with the addition of an ARL, it enables an obviously higher transmission efficiency. Numerical simulations show that the all-dielectric metamaterial can realize a high-performance cross-polarization conversion at the operation frequency. Several samples of the metamaterial polarization converter have been fabricated for test, and the experimental results agree well with the corresponding simulations.

As shown in Fig. 1(a), the all-dielectric metamaterial designed is made of pure silicon, and both working layers are composed of a periodic subwavelength pillar array based on a square unit cell. The HWP layer (HWPL) is based on elliptical pillars, and the ARL corresponds to square pillars. The specific structural parameters of the unit cells are defined in Figs. 1(b) and 1(c). For the HWPL, the period of the unit cell is P, the height of the elliptical pillar is H, and the major and minor axes are denoted by D and d, respectively; moreover, the major axis is at an angle of 45° relative to the x axis and is along the v axis. For the ARL, the period of the unit cell is p, and the height and side length of the square pillar are h and a, respectively. The thickness of the substrate is H_S. In our work, the size of the unit cells is much smaller than the wavelength of the incident THz wave, and hence, both the HWPL and ARL work in the effective medium regime.[35] Due to the anisotropy of the elliptical pillars of the HWPL, the phase difference is realized between the u and v polarizations, and similar to a traditional HWP, an x-polarized incidence along the z axis will be converted into a y-polarized output when the phase difference satisfies π at a specific frequency. As demonstrated in Ref. 36, a subwavelength square pillar array can achieve an antireflection effect and the ARL on the side opposite to the HWPL is used to improve the THz wave transmission, and it makes no contribution to the polarization conversion due to the isotropy of the square pillars.

For an HWP, we usually characterize its performance with the transmission and PCR, defined by

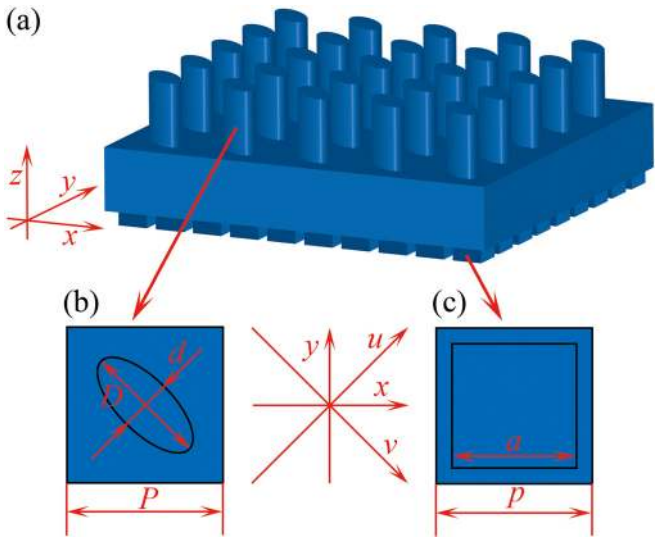

FIG. 1. Structure design of all-dielectric metamaterial HWP (a) and unit cells of HWPL (b) and ARL (c). A group of reference structural parameters have been chosen to be $P = 100\,\mu$m, elliptical pillar height $H = 300\,\mu$m, $D = 80\,\mu$m, $d = 35\,\mu$m, $p = 50\,\mu$m, $a = 40\,\mu$m, square pillar height $h = 45\,\mu$m, and substrate thickness $H_S = 1000\,\mu$m.

$$t_{xx} = E_x(f)/E_R(f), \tag{1a}$$

$$t_{xy} = E_y(f)/E_R(f), \tag{1b}$$

$$PCR = \frac{t_{xy}^2}{t_{xx}^2 + t_{xy}^2}, \tag{2}$$

where f is the frequency of the incident wave, $E_x(f)$ and $E_y(f)$ are the transmitted E-fields of the x- and y-components, respectively, and $E_R(f)$ is the reference E-field through air. Thus defined, t_{xx} and t_{xy} correspond to co- and cross-polarized transmissions, respectively. Further, the phase difference between u and v polarizations can be obtained by

$$\Delta\delta(f) = \delta_v(f) - \delta_u(f), \tag{3}$$

where $\delta_u(f)$ and $\delta_v(f)$ are the phases of u and v polarizations, respectively.

In order to investigate the properties of the metamaterial designed, the simulation of 3D-models with appropriate structural parameters has been done with *CST Microwave Studio*. The relative dielectric constant of silicon is set to 11.9. A linear x-polarized plane-wave along the z direction is used as incidence in the time-domain solver, and periodic boundary conditions are applied in both x and y directions to simplify the calculation. For reference, a group of structural parameters have been selected to be $P = 100\,\mu$m, $H = 300\,\mu$m, $D = 80\,\mu$m, $d = 35\,\mu$m, $p = 50\,\mu$m, $a = 40\,\mu$m, $h = 45\,\mu$m, and $H_S = 1000\,\mu$m.

As shown by the detailed simulations in Sec. 1 of the supplementary material, we first demonstrate that the substrate has no effect on the performance of the metamaterial and that there is no coupling between the two working layers. Then, the operation of the HWPL and ARL can be investigated independently, adjusted and optimized by changing the structural parameters. Further, it is demonstrated that the metamaterial HWP with an ARL has an obvious improvement of transmission at the operation frequency, but the ARL makes no contribution to the polarization conversion.

The simulation results for the reference structure, which is optimized for an operation frequency of 1 THz, are shown in Fig. 2. It can be seen that the transmission t_{xy} reaches a maximum of 90% at 1 THz, and meanwhile, the transmission t_{xx} is very close to zero in Fig. 2(a), which means that the x-polarized incidence can be converted into a y-polarized output at this operation frequency. According to Eq. (2), the PCR can reach almost 100% if the transmission t_{xx} is very close to zero, as the results show in Fig. 2(b). A PCR of 100% means that the output just has a polarized component in the y direction but there is no component in the x direction and further proves that the cross-polarization conversion is complete. Moreover, the metamaterial HWP induces a phase difference due to the anisotropy of the elliptical pillars, and the phase difference between the u and v polarizations is plotted in Fig. 2(c), where a value of π is observed at the operation frequency of 1 THz, just like a traditional HWP based on a birefringent material.

In order to visualize the polarization conversion process, the E-field amplitude distributions and phases for the reference structure at 1 THz are displayed in Fig. 3. Because of the periodic boundary conditions in the simulation, all these

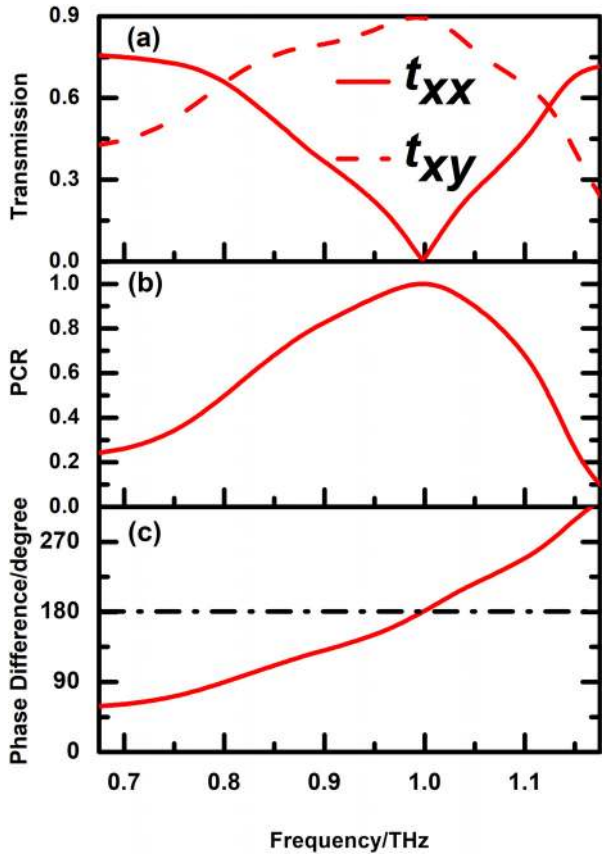

FIG. 2. Simulation results for the reference structure with parameters given in Fig. 1. (a) Transmission, (b) PCR, and (c) phase difference between *u* and *v* polarizations.

distributions are shown just for one unit cell. Figures 3(a)–3(d) correspond to the *y*-*z* cross-sections of the unit cell, and Figs. 3(e)–3(h) correspond to the *x*-*y* cross-sections at the arrow-indicated HWPL-substrate interface. From Figs. 3(a) and 3(c), one can clearly observe how the *x*-polarized incidence is gradually converted into a *y*-polarized output. Further, according to Figs. 3(e) and 3(g), the incidence has completed the conversion process at the arrow-indicated position, and Fig. 3(h) shows a uniform distribution of the *y*-polarization phase, which proves that the polarization

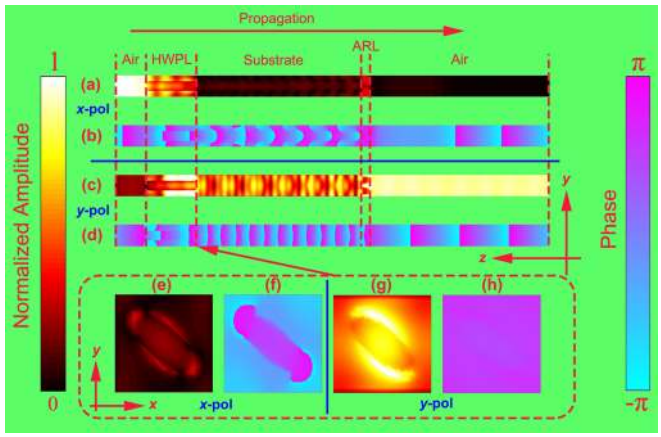

FIG. 3. Amplitude distributions and phases of polarized E-fields for the reference structure at 1 THz. (a)–(d) *y*-*z* cross-sections of the unit cell and (e) and (f) *x*-*y* cross-sections at the arrow-indicated position.

conversion relies on the HWPL. From the figures, one can also see how the wavelength changes in each region as determined by the (effective) material index. Incidentally, the bright and dark patterns observed in the substrate are caused by the interference between the incidence and reflected waves from the ARL-air interface. All these results prove that the metamaterial HWP designed can realize a high-performance cross-polarization conversion at a specific operation frequency.

With standard lithography, several metamaterial samples have been fabricated for experiment. The specific fabrication process is described in Sec. 2 of the supplementary material. Both the HWPL and ARL have a total area of $15 \times 15\,\mathrm{mm}^2$ etched on the opposite surfaces of a silicon wafer with a thickness of 1 mm, and the scanning electron microscopy images and the actual structural parameters of the samples have been measured and are given in Fig. S5 and Table S1 of the supplementary material. A THz time-domain spectroscopy system,[33] as schematically shown in Fig. S6 of the supplementary material, is used to characterize the properties of the samples. A femtosecond laser beam is split into two beams. One beam excites a photoconductive antenna to generate the linear-polarized THz incidence, and after going through the sample, the output THz beam carrying the material information reaches the detection photoconductive antenna. Another femtosecond beam is applied to detect the THz signal arriving at the detection antenna. In the set-up, four polarizers are used to control the polarization of the THz beams before being incident onto and after going through the sample. The THz signal is measured in the time-domain, and a Fourier transform is performed to convert it into the frequency domain. The material properties can thus be extracted by comparing the spectra of the THz beams going through the sample and through a reference. The experimental data have been collected and processed in this way. Moreover, in order to compare with the experiment, 3D-models with the actual structural parameters are built to do the simulations. The experimental and simulation results of sample 6 are compared in Fig. 4 as an example, where the actually measured parameters are $P = 100\,\mu\mathrm{m}$, $H = 274\,\mu\mathrm{m}$, $D = 82\,\mu\mathrm{m}$, $d = 39\,\mu\mathrm{m}$, $p = 50\,\mu\mathrm{m}$, $a = 40\,\mu\mathrm{m}$, and $h = 56\,\mu\mathrm{m}$, and the agreement is good. The results are similar and close to the reference structure described in Fig. 2; the transmissions t_{xy} reach about 80% at 1 THz, and meanwhile, the transmissions t_{xx} are very close to zero in Fig. 4(a). The PCR can reach almost 100% in Fig. 4(b). Furthermore, the phase differences between *u* and *v* polarizations are seen to be π at the operation frequency of 1 THz in Fig. 4(c). The discrepancies between experiment and simulation are believed to be mainly due to the inhomogeneity of the sample parameters. In spite of this, sample 6 can achieve a cross-polarization conversion with a cross-polarized transmission t_{xy} of about 80% and a PCR of almost 100% at the operation frequency of 1 THz. More results for different samples are compared in Fig. S7 of the supplementary material.

In conclusion, we have designed a transmissive all-dielectric metamaterial HWP with a double-working-layer structure. One of the layers consisting of an elliptical pillar array works as an HWP to enable polarization conversion of the incident THz wave, and the other composed of a square pillar array acts as an ARL to enhance the transmission.

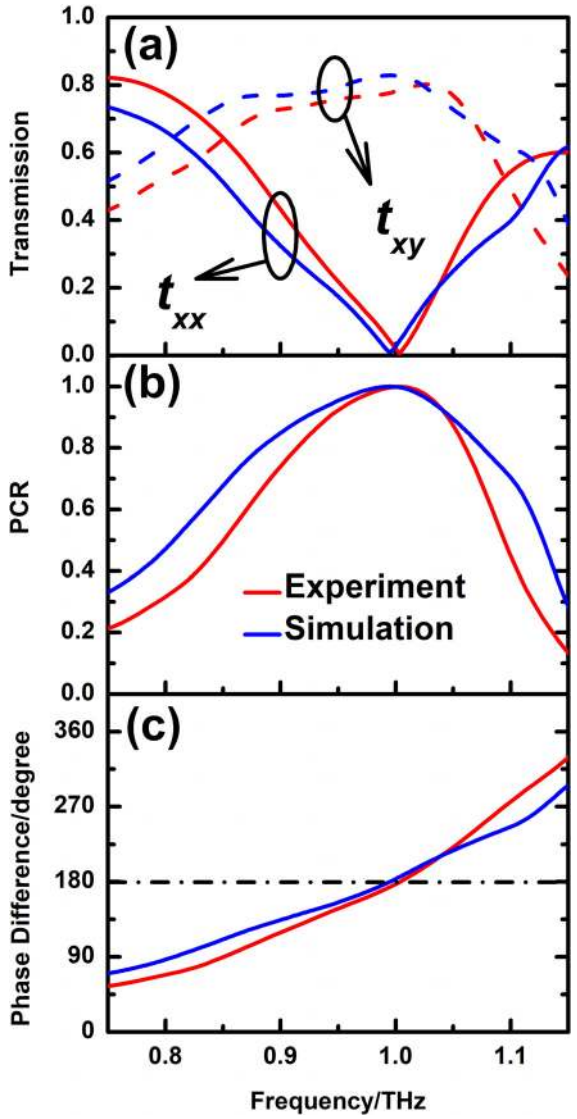

FIG. 4. Simulation and experimental results of sample 6. (a) Transmission, (b) PCR, and (c) phase difference between *u* and *v* polarizations.

Simulations show that the operation frequencies of both layers can be adjusted by the structural parameters. With appropriate structural design, the metamaterial HWP can realize a high performance cross-polarization conversion with a cross-polarized transmission of 90% at the operation frequency of 1 THz in simulation, and meanwhile, the PCR can reach almost 100%. Furthermore, several samples have been fabricated. The experimental results show a cross-polarized transmission of about 80% and a PCR of almost 100% and agree well with the corresponding simulations, proving our antireflection-assisted polarization convertor design. This high performance all-dielectric metamaterial HWP will be of great significance in future THz systems and applications.

See supplementary material for more details on numerical analysis of structural parameters, sample fabrication, experimental procedure, and comparison of data for more samples.

This work was supported by the National Basic Research Program of China (2014CB339800), the National Natural Science Foundation of China (61875150, 61622505, 61427814, 61377047, and 61420106006), the Program for Changjiang Scholars and Innovative Research Team in University (IRT13033), the Cooperative Innovation Center of Terahertz Science, and the U.S. National Science Foundation (ECCS-1232081).

[1]R. Fukasawa, IEEE Trans. Terahertz Sci. Technol. **5**, 1121 (2015), available at https://ieeexplore.ieee.org/document/7335441/.
[2]X. Yang, X. Zhao, K. Yang, Y. Liu, Y. Liu, W. Fu, and Y. Luo, Trends Biotechnol. **34**, 810 (2016).
[3]T. Nagatsuma, G. Ducournau, and C. C. Renaud, Nat. Photonics **10**, 371 (2016).
[4]M. T. Nouman, H. W. Kim, J. M. Woo, J. H. Hwang, D. Kim, and J. H. Jang, Sci. Rep. **6**, 26452 (2016).
[5]M. Rahm, J. S. Li, and W. J. Padilla, J. Infrared, Millimeter, Terahertz Waves **34**, 1 (2013).
[6]J. Liu, P. Li, Y. Chen, X. Song, Q. Mao, Y. Wu, F. Qi, B. Zheng, J. He, H. Yang, Q. Wen, and W. Zhang, Opt. Lett. **41**, 816 (2016).
[7]Y. Huang, S. Zhong, H. Yao, and D. Cui, IEEE Photonics J. **9**, 5900210 (2017).
[8]X. Chen and W. Fan, Sci. Rep. **7**, 2092 (2017).
[9]L. Chen, N. Xu, L. Singh, T. Cui, R. Singh, Y. Zhu, and W. Zhang, Adv. Opt. Mater. **5**, 1600960 (2017).
[10]L. Chen, Y. Wei, X. Zang, Y. Zhu, and S. Zhuang, Sci. Rep. **6**, 22027 (2016).
[11]J. He, P. Liu, Y. He, and Z. Hong, Appl. Opt. **51**, 776 (2012).
[12]L. Chen, Z. Cheng, J. Xu, X. Zang, B. Cai, and Y. Zhu, Opt. Lett. **39**, 4541 (2014).
[13]M. Wu, X. Zhao, J. Zhang, J. Schalch, G. Duan, K. Cremin, R. D. Averitt, and X. Zhang, Appl. Phys. Lett. **111**, 051101 (2017).
[14]Y. Cheng, Y. Nie, and R. Gong, Opt. Laser Technol. **48**, 415 (2013).
[15]X. Liu, K. Fan, I. V. Shadrivov, and W. J. Padilla, Opt. Express **25**, 191 (2017).
[16]W. S. L. Lee, S. Nirantar, D. Headland, M. Bhaskaran, S. Sriram, C. Fumeaux, and W. Withayachumnankul, Adv. Opt. Mater. **6**, 1700852 (2018).
[17]K. Wiesauer and C. Jördens, J. Infrared, Millimeter, Terahertz Waves **34**, 663 (2013).
[18]J. B. Masson and G. Gallot, Opt. Lett. **31**, 265 (2006).
[19]A. K. Kaveev, G. I. Kropotov, E. V. Tsygankova, I. A. Tzibizov, S. D. Ganichev, S. N. Danilov, P. Olbrich, C. Zoth, E. G. Kaveeva, A. I. Zhdanov, A. A. Ivanov, R. Z. Deyanov, and B. Redlich, Appl. Opt. **52**, B60–B69 (2013).
[20]D. Grischkowsky, S. Keiding, M. V. Exter, and C. Fattinger, J. Opt. Soc. Am. B **7**, 2006 (1990).
[21]S. B. Glybovski, S. A. Tretyakov, P. A. Belov, Y. S. Kivshar, and C. R. Simovski, Phys. Rep. **634**, 1 (2016).
[22]J. W. Stewart, G. M. Akselrod, D. R. Smith, and M. H. Mikkelsen, Adv. Mater. **29**, 1602971 (2017).
[23]D. Headland, E. Carrasco, S. Nirantar, W. Withayachumnankul, P. Gutruf, J. Schwarz, D. Abbott, M. Bhaskaran, S. Sriram, J. Perruisseau-Carrier, and C. Fumeaux, ACS Photonics **3**, 1019 (2016).
[24]I. Al-Naib and W. Withayachumnankul, J. Infrared, Millimeter, Terahertz Waves **38**, 1067 (2017).
[25]S. Liu and T. J. Cui, Adv. Opt. Mater. **5**, 1700624 (2017).
[26]R. Xia, X. Jing, X. Gui, Y. Tian, and Z. Hong, Opt. Mater. Express **7**, 977 (2017).
[27]Y. Nakata, Y. Taira, T. Nakanishi, and F. Miyamaru, Opt. Express **25**, 2107 (2017).
[28]L. Cong, W. Cao, Z. Tian, J. Gu, J. Han, and W. Zhang, New J. Phys. **14**, 115013 (2012).
[29]J. M. Woo, S. Hussain, and J. H. Jang, Sci. Rep. **7**, 42952 (2017).
[30]B. Vasić, D. C. Zografopoulos, G. Isić, R. Beccherelli, and R. Gajić, Nanotechnology **28**, 124002 (2017).
[31]D. Wang, L. Zhang, Y. Gu, M. Q. Mehmood, Y. Gong, A. Srivastava, L. Jian, T. Venkatesan, C. Qiu, and M. Hong, Sci. Rep. **5**, 15020 (2015).
[32]W. Liu, S. Chen, Z. Li, H. Cheng, P. Yu, J. Li, and J. Tian, Opt. Lett. **40**, 3185 (2015).
[33]M. Chen, F. Fan, S. T. Xu, and S. J. Chang, Sci. Rep. **6**, 38562 (2016).
[34]J. Zi, Q. Xu, Q. Wang, C. Tian, Y. Li, X. Zhang, J. Han, and W. Zhang, Opt. Commun. **416**, 130 (2018).
[35]J. D. Joannopoulos, S. G. Johnson, J. N. Winn, and R. D. Meade, *Photonic Crystals: Molding the Flow of Light*, 2nd ed. (Princeton University Press, Princeton, 2008).
[36]M. E. Motamedi, W. H. Southwell, and W. J. Gunning, Appl. Opt. **31**, 4371–4376 (1992).